Advances in the Stabilized Finite Point Method for Structural Mechanics

E. Oñate
F. Perazzo
J. Miquel

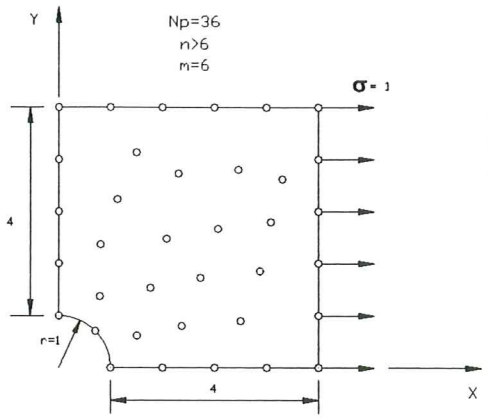

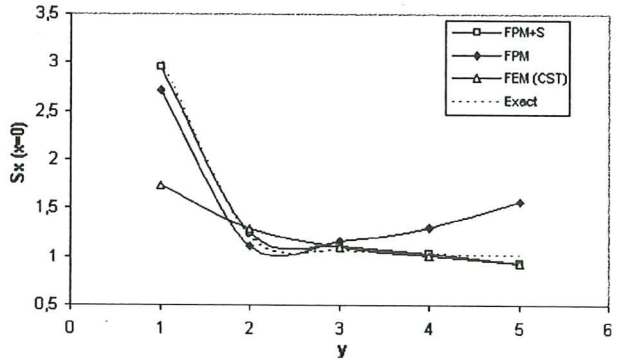

Publication CIMNE Nº 164, May 1999

Advances in the Stabilized Finite Point Method for Structural Mechanics

E. Oñate
F. Perazzo
J. Miquel

Publication CIMNE Nº 164, May 1999

International Center for Numerical Methods in Engineering
Gran Capitán s/n, 08034 Barcelona, Spain

ECCM '99
European Conference on
Computational Mechanics
August 31 – September 3
München, Germany

ADVANCES IN THE STABILIZED FINITE POINT METHOD FOR STRUCTURAL MECHANICS

E. Oñate, F. Perazzo and J. Miquel
International Centre for Numerical Methods in Engineering
Universidad Politécnica de Cataluña
Gran Capitán s/n, 08034 Barcelona, Spain
e–mail: cimne@etseccpb.upc.es

Key words: Finite Point Method, Meshless Method, Structural Mechanics.

Abstract. *The basis of the finite point method for the fully meshless solution of structural mechanics problems is described. A new stabilization technique based on a finite increment calculus procedure is used. The efficiency and accuracy of the stabilized finite point method in the meshless analysis of simple structural problems is shown in two examples of applications.*

1 Advances in the finite point method for mesh free analysis in fluid and solid mechanics

Mesh free techniques have become quite popular in computational mechanics. A family of mesh free methods is based on smooth particle hydrodynamic procedures. [1,2]. These techniques, also called free lagrangian methods, are typically used for problems involving large motions of solids and moving free surfaces in fluids. A second class of mesh free methods derive from generalized finite difference (GFD) techniques [3,4]. Here the approximation around each point is typically defined in terms of Taylor series expansions and the discrete equations are found by using point collocation. Among a third class of mesh free techniques we find the so called diffuse element (DE) method [5], the element free Galerking (EFG) method [6,7] and the reproducing kernel particle (RKP) method [8,9]. These three methods use local interpolations for defining the approximate field around a point in terms of values in adjacent points, whereas the discretized system of equations is typically obtained by integrating the Galerkin variational form over a suitable background grid.

The *finite point method* (FPM) proposed in [10–13] is a truly meshless procedure. The approximation around each point is obtained by using standard moving least square techniques similarly as in DE and EFG methods. The discrete system of equations is obtained by sampling the governing differential equations at each point as in GFD methods.

The basis of the success of the FPM for solid and fluid mechanics applications is the *stabilization* of the discrete differential equations. The stable form found by the *finite element calculus* procedure presented in [14–17] corrects the errors introduced by the point collocation procedure, mainly next to the boundary segments. In addition, it introduces the necessary stabilization for treating high convection effects and it also allows equal order velocity-pressure interpolations in fluid flow problems [17].

The content of the paper is structured as follows. In next section on the basis of the FPM approximation is presented. The discretization of the equilibrium equations in solid mechanics using a stabilized finite point method is described next. The efficiency of the stabilized FPM is verified in two applications to simple solid mechanics problems.

1.1 Interpolation in the FPM

Let Ω_i be the interpolation domain (cloud) of a function $u(x)$ and let s_j with $j = 1, 2, \cdots, n$ be a collection of n points with coordinates $x_j \in \Omega_i$. The unknown function u may be approximated within Ω_i by

$$u(x) \cong \hat{u}(x) = \sum_{l=1}^{m} p_l(x)\alpha_l = \mathbf{p}(x)^T \boldsymbol{\alpha} \tag{1}$$

where $\boldsymbol{\alpha} = [\alpha_1, \alpha_2, \cdots \alpha_m]^T$ and vector $\mathbf{p}(x)$ contains typically monomials, hereafter termed "base interpolating functions", in the space coordinates ensuring that the basis is complete. For a 2D problem we can specify

$$\mathbf{p} = [1, x, y]^T \quad \text{for} \quad m = 3 \tag{2}$$

and

$$\mathbf{p} = [1, x, y, x^2, xy, y^2]^T \quad \text{for} \quad m = 6 \qquad \text{etc.} \tag{3}$$

Function $u(x)$ can now be sampled at the n points belonging to Ω_i giving

$$\mathbf{u}^h = \begin{Bmatrix} u_1^h \\ u_2^h \\ \vdots \\ u_n^h \end{Bmatrix} \cong \begin{Bmatrix} \hat{u}_1 \\ \hat{u}_2 \\ \vdots \\ \hat{u}_n \end{Bmatrix} = \begin{Bmatrix} \mathbf{p}_1^T \\ \mathbf{p}_2^T \\ \vdots \\ \mathbf{p}_n^T \end{Bmatrix} \boldsymbol{\alpha} = \mathbf{C}\boldsymbol{\alpha} \tag{4}$$

where $u_j^h = u(x_j)$ are the unknown but sought for values of function u at point j, $\hat{u}_j = \hat{u}(x_j)$ are the approximate values, and $\mathbf{p}_j = \mathbf{p}(x_j)$.

In the FE approximation the number of points is chosen so that $m = n$. In this case $\mathbf{C}$ is a square matrix. The procedure leads to the standard shape functions in the FEM [18].

If $n > m$, $\mathbf{C}$ is no longer a square matrix and the approximation can not fit all the u_j^h values. This problem can be simply overcome by determining the $\hat{u}$ values by minimizing the sum of the square distances of the error at each point weighted with a function $\varphi(x)$ as

$$J = \sum_{j=1}^{n} \varphi(x_j)\left(u_j^h - \hat{u}(x_j)\right)^2 = \sum_{j=1}^{n} \varphi(x_j)\left(u_j^h - \mathbf{p}_j^T\boldsymbol{\alpha}\right)^2 \tag{5}$$

with respect to the $\boldsymbol{\alpha}$ parameters. Note that for $\varphi(x) = 1$ the standard least square (LSQ) method is reproduced.

Function $\varphi(x)$ is usually built in such a way that it takes a unit value in the vicinity of the point i typically called "star node" where the function (or its derivatives) are to be computed and vanishes outside a region Ω_i surrounding the point. The region Ω_i can be used to define the number of sampling points n in the interpolation region. A typical choice for $\varphi(x)$ is the normalized Gaussian function and this has been chosen in the examples shown in the paper. Of course $n \geq m$ is always required in the sampling region and if equality occurs no effect of weighting is present and the interpolation is the same as in the LSQ scheme.

Standard minimization of eq.(5) with respect to $\boldsymbol{\alpha}$ gives

$$\boldsymbol{\alpha} = \bar{\mathbf{C}}^{-1}\mathbf{u}^h \quad , \quad \bar{\mathbf{C}}^{-1} = \mathbf{A}^{-1}\mathbf{B} \tag{6}$$

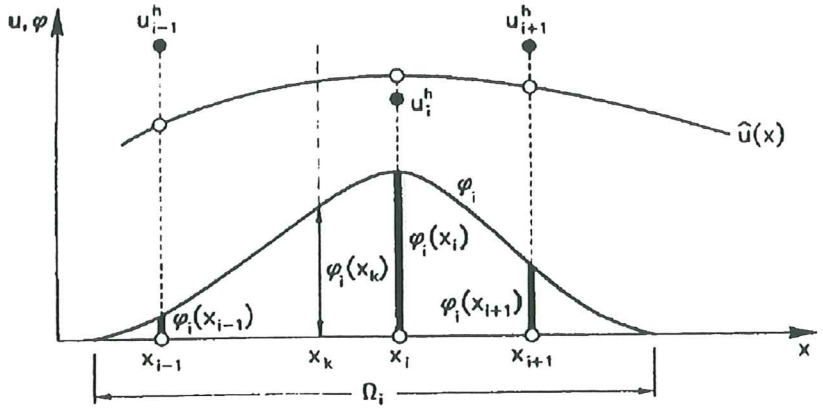

Figure 1: Fixed weighing least square procedure.

$$\begin{aligned} \mathbf{A} &= \sum_{j=1}^{n} \varphi(x_j)\mathbf{p}(x_j)\mathbf{p}^T(x_j) \\ \mathbf{B} &= [\varphi(x_1)\mathbf{p}(x_1), \varphi(x_2)\mathbf{p}(x_2), \cdots, \varphi(x_n)\mathbf{p}(x_n)] \end{aligned} \tag{7}$$

The final approximation is obtained by substituting $\boldsymbol{\alpha}$ from eq.(6) into (1) giving

$$\hat{u}(x) = \mathbf{p}^T\bar{\mathbf{C}}^{-1}\mathbf{u}^h = \mathbf{N}^T\mathbf{u}^h = \sum_{j=1}^{n} N_j^i u_j^h \tag{8}$$

where the "shape functions" are

$$N_j^i(x) = \sum_{l=1}^{m} p_l(x)\bar{C}_{lj}^{-1} = \mathbf{p}^T(x)\bar{\mathbf{C}}^{-1} \tag{9}$$

It must be noted that accordingly to the least square character of the approximation

$$u(x_j) \simeq \hat{u}(x_j) \neq u_j^h \tag{10}$$

i.e. the local values of the approximating function do not fit the nodal unknown values (Figure 1). Indeed $\hat{u}$ is the true approximation for which we shall seek the satisfaction of the differential equation and the boundary conditions and u_j^h are simply the unknown parameters sought.

The weighted least square approximation described above depends on a great extend on the shape and the way to apply the weighting function. The simplest way is to define a fixed function $\varphi(x)$ for each of the Ω_i interpolation domains [11,12].

Let $\varphi_i(x)$ be a weighting functions satisfying

$$\begin{aligned} \varphi_i(x_i) &= 1 \\ \varphi_i(x) &\neq 0 \qquad x \in \Omega_i \\ \varphi_i(x) &= 0 \qquad x \notin \Omega_i \end{aligned} \tag{11}$$

Then the minimization square distance becomes

$$J_i = \sum_{j=1}^{n} \varphi_i(x_j)(u_j^h - \hat{u}(x_j))^2 \quad \text{minimum} \tag{12}$$

The expression of matrices **A** and **B** coincide with eq.(7) with $\varphi(x_j) = \varphi_i(x_j)$

Note that according to (1), the approximate function $\hat{u}(x)$ is defined in each interpolation domain Ω_i. In fact, different interpolation domains can yield different shape functions N_j^i. As a consequence a point belonging to two or more overlapping interpolation domains has different values of the shape functions which means that $N_j^i \neq N_j^k$. The interpolation is now multivalued within Ω_i and, therefore for any useful approximation a decision must be taken limiting the choice to a single value. Indeed, the approximate function $\hat{u}(x)$ will be typically used to provide the value of the unknown function $u(x)$ and its derivatives in only specific regions within each interpolation domain. For instance by using point collocation we may limit the validity of the interpolation to a single point x_i. It is precisely in this context where we have found this meshless method to be more useful for practical purposes [10–13].

1.2 Discretization of governing equations

Let us assume a problem governed by the following set of differential equations

$$A(u_j) = 0 \qquad \text{in } \Omega \tag{13a}$$

with boundary conditions

$$u_j - \bar{u}_j = 0 \qquad \text{on } \Gamma_u \tag{13b}$$

$$B(u_j) = 0 \qquad \text{on } \Gamma_t \tag{13c}$$

In above A is a differential operator defining the governing differential equations to be satisfied on the domain Ω with boundary $\Gamma = \Gamma_t \cup \Gamma_\phi$, B is the differential operator defining the boundary conditions at the Neumann boundary Γ_t, u_j are the unknown variables with prescribed values $\bar{u}_j$ at the boundary Γ_u, $j = 1, 2, \cdots, N_v$ where N_v is the number of variables. In solid mechanics application u_j are the displacements and A and B are the equilibrium equations to be satisfied in the domain Ω and the boundary Γ_t where tractions are prescribed respectiveley.

The successful application of the FPM in fluid and solid mechanics requires the "stabilization" of the discrete form. The reasons for this stabilization in fluid problems is due to

the effect of convection terms and the need to satisfy the incompressibility requirements are due to the need for improving the satisfaction of the equilibrium equations (13a) and (13c) over a "cloud" when using a point collocation procedure.

A stabilized form of the differential equations [(13) can be found by using the *finite increment calculus* (FIC) procedure described in [14–17]. The FIC method is based on imposing the balance laws typical of solid and fluid mechanics over a domain of finite size and retaining higher order terms in the standard Taylor series expansion used to approximate the unknown field over the balance domain. The stabilized form of eqs. (13) reads

$$\begin{aligned} A - \underline{\frac{1}{2} h_j \frac{\partial A}{\partial x_j}} &= 0 \qquad \text{in } \Omega \\ u_j - \bar{u}_j &= 0 \qquad \text{on } \Gamma_u \\ B - \underline{\frac{1}{2} h_j n_j A} &= 0 \qquad \text{on } \Gamma_t \end{aligned} \tag{14}$$

where n_j are the components of the unit normal to the boundary Γ_t and h_j are the dimensions of the balance domain (also called characteristic length parameters). The underlined terms in eq.(14) introduce the necessary stabilization in the governing equations at discrete level. It can be shown that eqs.(14) are the starting point for deriving many well known stabilized numerical methods typically used in computational fluid dynamic problems [14–17]. The stabilized equations (14) have also been found useful for enhanced application of the FPM in fluid mechanics [12,13]. The efficiency of this stabilization procedure for the application of the FPM in solid mechanics will be shown in the examples presented in next section.

The discretized system of equations in the FPM is found by substituting the approximation (8) into eqs.(14) and *collocating* the differential equations at each point in the analysis domain. This gives

$$\begin{aligned} &\left[A(\hat{u}_j) - \frac{1}{2} h_j \frac{\partial}{\partial x_j} A(\hat{u}_j) \right]_k = 0 \qquad k = 1, 2 \cdots N_t \\ &[\hat{u}_j]_s - \bar{u}_j = 0 \qquad s = 1, 2 \cdots N_s \\ &\left[B(\hat{u}_j) - \frac{1}{2} h_j n_j A(\hat{u}_j) \right]_p = 0 \qquad p = 1, 2 \cdots N_t \end{aligned} \tag{15}$$

In above N_t is the number of points within the domain Ω and N_s and N_t are the points located on the boundaries Γ_u and Γ_t, respectively.

The discretized system of equations (15) can be written in the standard matrix form

$$\mathbf{K}\mathbf{u}^h = \mathbf{f} \tag{16}$$

from where the values of the nodal parameters u_i^h can be found.

Details of the implementation of the boundary conditions on the Dirichlet boundary Γ_t are given in [11,12].

The computation of the characteristic length parameters h_i follows the procedure explained in [13–17]. In the examples shown in the paper using quadratic base functions, the value $h_i = d_i^{\min}$ has been chosen where $d_i^{\min}$ is the closest distance from a star node in a cloud to its closest neighbour.

Further details on the FPM can be found in [10–13].

1.3 Example 1. Analysis of a simple supported beam under distributed loading

Figure 2 shows the geometry of the beam, the mechanical properties and the uniform distribution of 51 points. A uniform load acting on the upper edge is considered. A quadratic interpolation ($m = 6$) for the displacement variables has been chosen. Numerical results for the beam deflection and the horizontal stress distribution are shown. The same problem has been analyzed with the FEM using a structured mesh of 68 linear plane stress triangles (CST element) based on the same point distribution. Nodal stresses have been obtained by standard nodal averaging of element values. Comparison of the errors for the control deflection and the maximum σ_x stress gives some advantage to the stabilized FPM results (see Table 1).

Numerical results for grid of 51 points (68 CST finite elements)			
Central deflection error		Error in maximum σ_x stress	
FPM+S	FEM	FPM+S	FEM
19%	21%	19%	38%

Table 1: Simple supported beam. Numerical results for grid of 51 points (68 CST finite elements)

The convergence of the maximum horizontal stress and the maximum deflection value with the number of points is shown in the lower part of Figure 2, respectively. Results, listed as FPM+S, correspond to those obtained with the stabilized FPM described in the paper, whereas those listed as FPM were obtained neglecting the stabilization terms (i.e. the terms involving the characteristic lenght parameters in eqs.(14) and (15)). Note the benefitial effect of the stabilization terms leading to results which are more accurate than those obtained by the standard FEM in all cases.

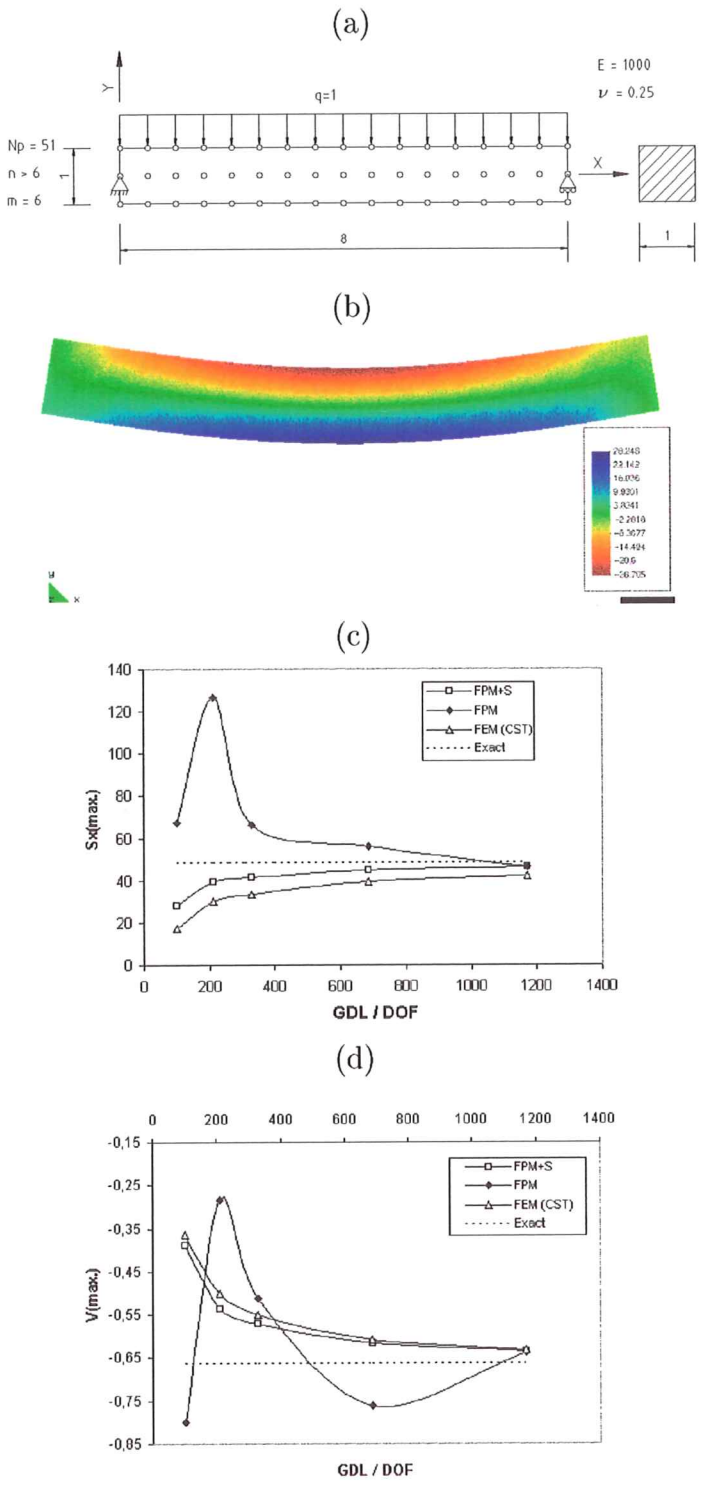

Figure 2: Simple supported beam analyzed with FPM and CST finite elements. (a) Beam geometry and loading. (b) Structured grid of 51 points. Convergence of maximum horizontal stress (c) and the maximum deflection (d) with the number of degrees of freedom. Exact solution refers to classical beam theory [19].

1.4 Example 2. Square plate with circular hole under tension

Figure 3 shows the geometry of the plate and the loading. One quater of the plate is analyzed only due to symmetry. The problem has been solved with the FPM using two unstructured grids of 36 and 60 points. Contours of horizontal stress obtained with the stabilized FPM are shown in Figures 3 and 4 for the two grids. Results for the maximum horizontal stress at the upper tip of the hole obtained with the stabilized FPM are very accurate. This compares very favourably with the error obtained with the FEM using an unstructured mesh of CST elements. The distribution of the maximum horizontal stress along the line $x = 0$ is also shown in Figure 3 for the two grids studied. Note the greater accuracy of the stabilized FPM solution versus the standard FPM and FEM solutions (see Table 2).

36 points - 50 CST Triangles		60 points - 94 CST Triangles	
FPM+S	FEM	FPM+S	FEM
6%	38%	1,5%	21%

Table 2: Square plate with circular hole. Error in maximum horizontal stress obtained with the stabilized finite point method (FPM+S) and the finite element method (FEM)

CONCLUSIONS

The stabilized FPM is a promising numerical method for the meshless solution of problems in solid mechanics. Results for the two problems analyzed with the stabilized FPM yielded a higher accuracy than those obtained with standard FEM. The accuracy was remarkably higher for the maximum stress values. The optimal selection of the stabilization parameters and the validation of the stabilized FPM for problems involving heterogeneous materials and 3D geometries are the main challenges in the extension and validation of the new meshless procedure.

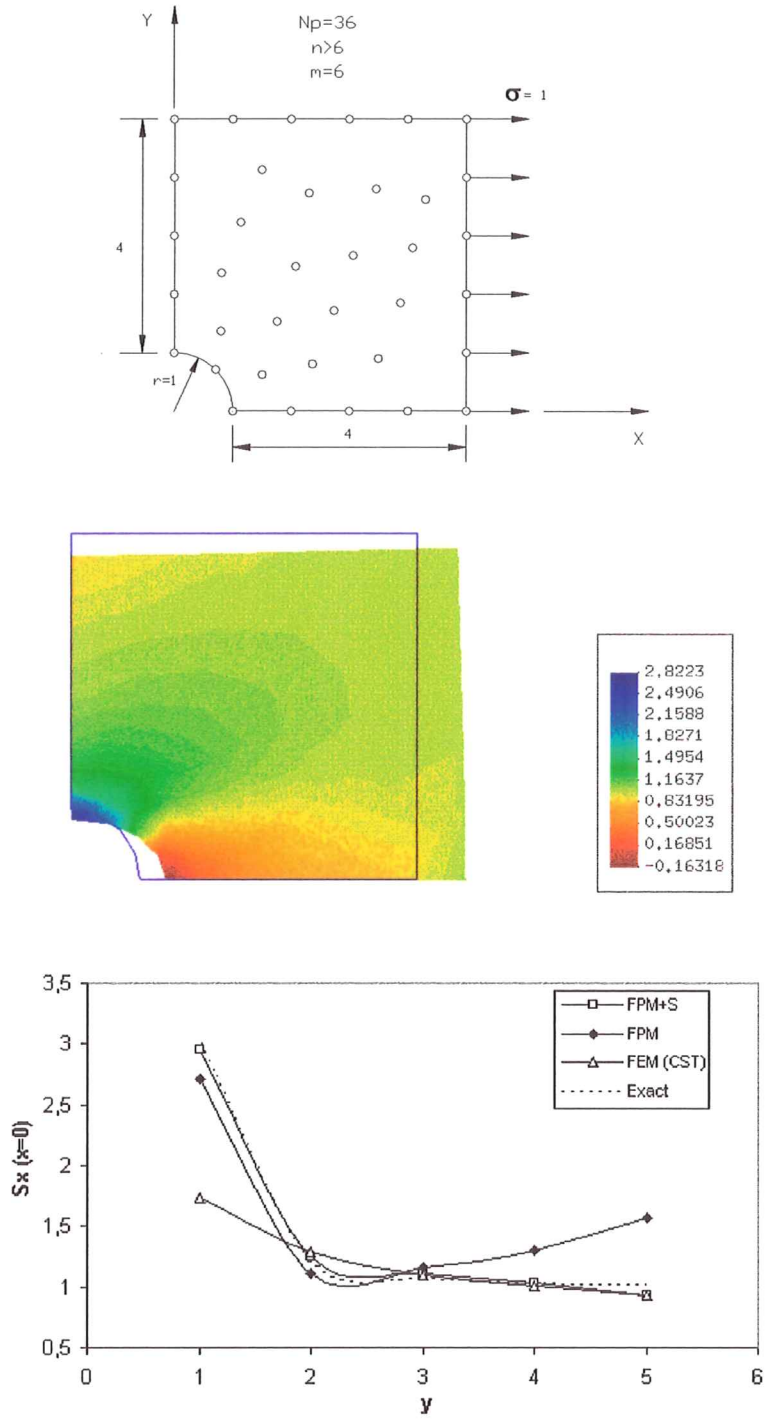

Figure 3: Square plate with circular hole under tension analyzed with FPM and FEM (CST elements) ($E = 1000$, $\nu = 0.3$). Plate geometry and loading. Unstructured grid of 36 points. Stress contours displayed over the deformed shape for the two grids studied. Distribution of maximum horizontal stress along the line $x = 0$ for the two grids studied.

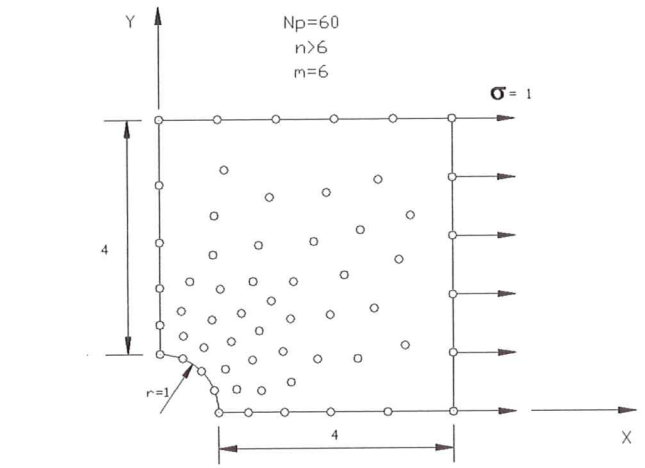

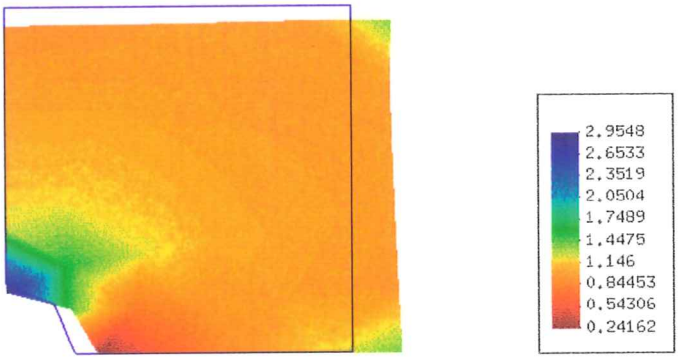

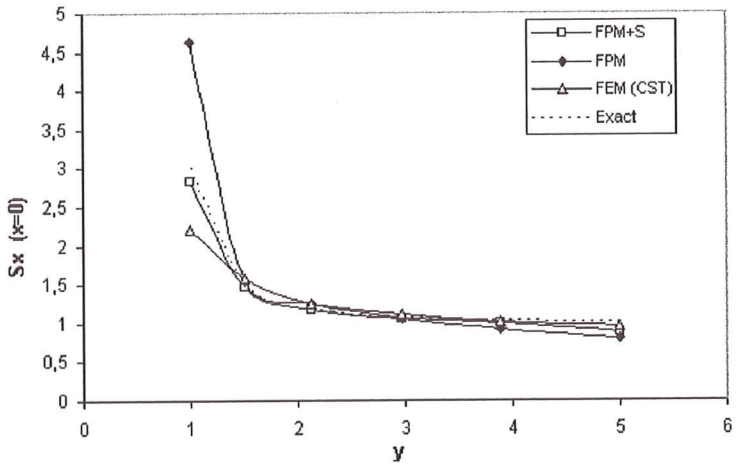

Figure 4: Square plate with circular hole under tension analyzed with FPM and FEM (CST elements) ($E = 1000$, $\nu = 0.3$). Plate geometry and loading. Unstructured grid of 60 points. Stress contours displayed over the deformed shape for the two grids studied. Distribution of maximum horizontal stress along the line $x = 0$ for the two grids studied.

References

[1] J.J. Monaghan. *Smoothed particle hydrodynamics: Some recent improvement and applications.* Annu. Rev. Astron. Physics, **30**, 543, (1992).

[2] P.W. Randles and L.D. Libersky. *Smoothed particle hydrodynamics: Some recent improvement and applications.* Appl. Mech. Engng., **139**, 175, (1996).

[3] N. Perrone and R. Kao. *A general finite difference method for arbitrary meshes.* Comp. Struct, **5**, 45-47, (1975).

[4] T. Liszka and J. Orkisz. *The finite difference method at arbitrary irregular grids and its application in applied mechanics.* Comp. Struct., **11**, 83-95, (1980).

[5] B. Nayroles, G. Touzot and P. Villon. *Generalizing the FEM: Diffuse approximation and diffuse elements.* Comput. Mechanics, **10**, 307-18, (1992).

[6] T. BELYTSCHKO, Y. LU and L. GU. *Element free Galerkin methods.* Int. J. Num. Meth. Engng., **37**, 229-56, (1994).

[7] J. Dolbow and T. Belytschko. *An introduction to programming the meshless element free Galerkin method.* Archives of Comput. Meth. in Engng., **5** (3), 207–241, (1998).

[8] W.K. Liu, S. Jun, S. LI, J. Adee and T. Belytschko. *Reproducing Kernel particle methods for structural dynamics.* Int. J. Num. Meth. Engng., **38**, 1655–1679, (1995).

[9] W.K. Liu, Y Chen, s. Jun, J.s. Chen, T. Belytschko, C. Pan, R.A. Uras and C.T. Chang. *Overview and applications of the Reproducing Kernel particle method.* Archives of Comput. Meth. in Engng., Vol. **3**(1), 3–80, (1996).

[10] E. Oñate, S. Idelsohn, O.C. Zienkiewicz and T. Fisher. *A finite point method for analysis of fluid flow problems.* Proceedings of the 9th Int. Conference on Finite Element Methods in Fluids, Venize, Italy, 15-21, October (1995).

[11] E. Oñate, S. Idelsohn, O.C. Zienkiewicz and R.L. Taylor. *A finite point method in computational mechanics. Applications to convective transport and fluid flow.* Int. J. Num. Meth. Engng., Vol. **39**, 3839–3866, (1996).

[12] E. Oñate, S. Idelsohn, O.C. Zienkiewicz and R.L. Taylor. *A stabilized finite point method for analysis of fluid mechanics's problems.* Comput. Meth. in Appl. Engng., Vol. **139**, 1-4, pp. 315–347, (1996).

[13] E. Oñate and S. Idelsohn. *A mesh free finite point method for advective-diffusive transport and fluid flow problems.* Computational Mechanics, **21**, 283–292, (1988).

[14] E. Oñate. *Derivation of stabilized equations for advective-diffusive transport and fluid flow problems.* Comput. Meth. Appl. Mech. Engng., Vol. 151, 1-2, pp. 233–267, (1998).

[15] E. Oñate, J. García and S. Idelsohn. *Computation of the stabilization parameter for the finite element solution of advective-diffusive problems.* Int. J. Num. Meth. Fluids, Vol. 25, pp. 1385–1407, (1997).

[16] E. Oñate, J. García and S. Idelsohn. *An Alpha-adaptive approach for stabilized finite element solution of advective-diffusive problems with sharp gradients.* New Adv. in Adaptive Comp. Met. in Mech., P. Ladeveze and J.T. Oden (Eds.), Elsevier, (1998).

[17] E. Oñate. *A finite element method for incompressible viscous flows using a finite increment calculus formulation.* Research Report N. 150, CIMNE, Barcelona, January (1999).

[18] O.C. Zienkiewicz and R.L. Taylor. *The finite element method.* 4th Edition, Vol. 1, McGraw Hill, (1989).

[19] S.P. Timoshenko and J.N. Goodier. *Theory of elasticity.* 3rd. Edition, McGraw Hill, (1970).

Advances in the Stabilized Finite Point Method for Structural Mechanics

E. Oñate
F. Perazzo
J. Miquel

Publication CIMNE Nº 164, May 1999

International Center for Numerical Methods in Engineering
Gran Capitán s/n, 08034 Barcelona, Spain

ECCM '99
European Conference on
Computational Mechanics
August 31 – September 3
München, Germany

ADVANCES IN THE STABILIZED FINITE POINT METHOD FOR STRUCTURAL MECHANICS

E. Oñate, F. Perazzo and J. Miquel
International Centre for Numerical Methods in Engineering
Universidad Politécnica de Cataluña
Gran Capitán s/n, 08034 Barcelona, Spain
e–mail: cimne@etseccpb.upc.es

Key words: Finite Point Method, Meshless Method, Structural Mechanics.

Abstract. *The basis of the finite point method for the fully meshless solution of structural mechanics problems is described. A new stabilization technique based on a finite increment calculus procedure is used. The efficiency and accuracy of the stabilized finite point method in the meshless analysis of simple structural problems is shown in two examples of applications.*

1 Advances in the finite point method for mesh free analysis in fluid and solid mechanics

Mesh free techniques have become quite popular in computational mechanics. A family of mesh free methods is based on smooth particle hydrodynamic procedures. [1,2]. These techniques, also called free lagrangian methods, are typically used for problems involving large motions of solids and moving free surfaces in fluids. A second class of mesh free methods derive from generalized finite difference (GFD) techniques [3,4]. Here the approximation around each point is typically defined in terms of Taylor series expansions and the discrete equations are found by using point collocation. Among a third class of mesh free techniques we find the so called diffuse element (DE) method [5], the element free Galerking (EFG) method [6,7] and the reproducing kernel particle (RKP) method [8,9]. These three methods use local interpolations for defining the approximate field around a point in terms of values in adjacent points, whereas the discretized system of equations is typically obtained by integrating the Galerkin variational form over a suitable background grid.

The *finite point method* (FPM) proposed in [10–13] is a truly meshless procedure. The approximation around each point is obtained by using standard moving least square techniques similarly as in DE and EFG methods. The discrete system of equations is obtained by sampling the governing differential equations at each point as in GFD methods.

The basis of the success of the FPM for solid and fluid mechanics applications is the *stabilization* of the discrete differential equations. The stable form found by the *finite element calculus* procedure presented in [14–17] corrects the errors introduced by the point collocation procedure, mainly next to the boundary segments. In addition, it introduces the necessary stabilization for treating high convection effects and it also allows equal order velocity-pressure interpolations in fluid flow problems [17].

The content of the paper is structured as follows. In next section on the basis of the FPM approximation is presented. The discretization of the equilibrium equations in solid mechanics using a stabilized finite point method is described next. The efficiency of the stabilized FPM is verified in two applications to simple solid mechanics problems.

1.1 Interpolation in the FPM

Let Ω_i be the interpolation domain (cloud) of a function $u(x)$ and let s_j with $j = 1, 2, \cdots, n$ be a collection of n points with coordinates $x_j \in \Omega_i$. The unknown function u may be approximated within Ω_i by

$$u(x) \cong \hat{u}(x) = \sum_{l=1}^{m} p_l(x)\alpha_l = \mathbf{p}(x)^T \boldsymbol{\alpha} \tag{1}$$

where $\boldsymbol{\alpha} = [\alpha_1, \alpha_2, \cdots \alpha_m]^T$ and vector $\mathbf{p}(x)$ contains typically monomials, hereafter termed "base interpolating functions", in the space coordinates ensuring that the basis is complete. For a 2D problem we can specify

$$\mathbf{p} = [1, x, y]^T \quad \text{for} \quad m = 3 \tag{2}$$

and

$$\mathbf{p} = [1, x, y, x^2, xy, y^2]^T \quad \text{for} \quad m = 6 \qquad \text{etc.} \tag{3}$$

Function $u(x)$ can now be sampled at the n points belonging to Ω_i giving

$$\mathbf{u}^h = \begin{Bmatrix} u_1^h \\ u_2^h \\ \vdots \\ u_n^h \end{Bmatrix} \cong \begin{Bmatrix} \hat{u}_1 \\ \hat{u}_2 \\ \vdots \\ \hat{u}_n \end{Bmatrix} = \begin{Bmatrix} \mathbf{p}_1^T \\ \mathbf{p}_2^T \\ \vdots \\ \mathbf{p}_n^T \end{Bmatrix} \boldsymbol{\alpha} = \mathbf{C}\boldsymbol{\alpha} \tag{4}$$

where $u_j^h = u(x_j)$ are the unknown but sought for values of function u at point j, $\hat{u}_j = \hat{u}(x_j)$ are the approximate values, and $\mathbf{p}_j = \mathbf{p}(x_j)$.

In the FE approximation the number of points is chosen so that $m = n$. In this case $\mathbf{C}$ is a square matrix. The procedure leads to the standard shape functions in the FEM [18].

If $n > m$, $\mathbf{C}$ is no longer a square matrix and the approximation can not fit all the u_j^h values. This problem can be simply overcome by determining the $\hat{u}$ values by minimizing the sum of the square distances of the error at each point weighted with a function $\varphi(x)$ as

$$J = \sum_{j=1}^{n} \varphi(x_j)\big(u_j^h - \hat{u}(x_j)\big)^2 = \sum_{j=1}^{n} \varphi(x_j)\big(u_j^h - \mathbf{p}_j^T\boldsymbol{\alpha}\big)^2 \tag{5}$$

with respect to the $\boldsymbol{\alpha}$ parameters. Note that for $\varphi(x) = 1$ the standard least square (LSQ) method is reproduced.

Function $\varphi(x)$ is usually built in such a way that it takes a unit value in the vicinity of the point i typically called "star node" where the function (or its derivatives) are to be computed and vanishes outside a region Ω_i surrounding the point. The region Ω_i can be used to define the number of sampling points n in the interpolation region. A typical choice for $\varphi(x)$ is the normalized Gaussian function and this has been chosen in the examples shown in the paper. Of course $n \geq m$ is always required in the sampling region and if equality occurs no effect of weighting is present and the interpolation is the same as in the LSQ scheme.

Standard minimization of eq.(5) with respect to $\boldsymbol{\alpha}$ gives

$$\boldsymbol{\alpha} = \bar{\mathbf{C}}^{-1}\mathbf{u}^h \qquad , \qquad \bar{\mathbf{C}}^{-1} = \mathbf{A}^{-1}\mathbf{B} \tag{6}$$

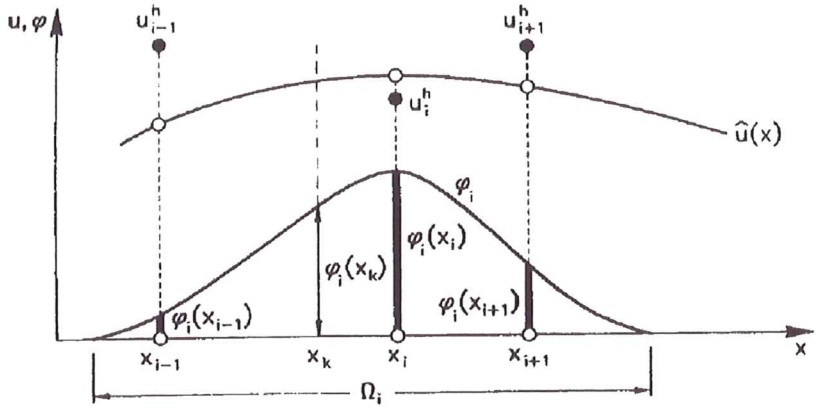

Figure 1: Fixed weighing least square procedure.

$$\begin{aligned} \mathbf{A} &= \sum_{j=1}^{n} \varphi(x_j)\mathbf{p}(x_j)\mathbf{p}^T(x_j) \\ \mathbf{B} &= \left[\varphi(x_1)\mathbf{p}(x_1), \varphi(x_2)\mathbf{p}(x_2), \cdots, \varphi(x_n)\mathbf{p}(x_n)\right] \end{aligned} \tag{7}$$

The final approximation is obtained by substituting $\boldsymbol{\alpha}$ from eq.(6) into (1) giving

$$\hat{u}(x) = \mathbf{p}^T\bar{\mathbf{C}}^{-1}\mathbf{u}^h = \mathbf{N}^T\mathbf{u}^h = \sum_{j=1}^{n} N_j^i u_j^h \tag{8}$$

where the "shape functions" are

$$N_j^i(x) = \sum_{l=1}^{m} p_l(x)\bar{C}_{lj}^{-1} = \mathbf{p}^T(x)\bar{\mathbf{C}}^{-1} \tag{9}$$

It must be noted that accordingly to the least square character of the approximation

$$u(x_j) \simeq \hat{u}(x_j) \neq u_j^h \tag{10}$$

i.e. the local values of the approximating function do not fit the nodal unknown values (Figure 1). Indeed $\hat{u}$ is the true approximation for which we shall seek the satisfaction of the differential equation and the boundary conditions and u_j^h are simply the unknown parameters sought.

The weighted least square approximation described above depends on a great extend on the shape and the way to apply the weighting function. The simplest way is to define a fixed function $\varphi(x)$ for each of the Ω_i interpolation domains [11,12].

Let $\varphi_i(x)$ be a weighting functions satisfying

$$\begin{aligned} \varphi_i(x_i) &= 1 \\ \varphi_i(x) &\neq 0 \qquad x \in \Omega_i \\ \varphi_i(x) &= 0 \qquad x \notin \Omega_i \end{aligned} \tag{11}$$

Then the minimization square distance becomes

$$J_i = \sum_{j=1}^{n} \varphi_i(x_j)(u_j^h - \hat{u}(x_j))^2 \quad \text{minimum} \tag{12}$$

The expression of matrices **A** and **B** coincide with eq.(7) with $\varphi(x_j) = \varphi_i(x_j)$

Note that according to (1), the approximate function $\hat{u}(x)$ is defined in each interpolation domain Ω_i. In fact, different interpolation domains can yield different shape functions N_j^i. As a consequence a point belonging to two or more overlapping interpolation domains has different values of the shape functions which means that $N_j^i \neq N_j^k$. The interpolation is now multivalued within Ω_i and, therefore for any useful approximation a decision must be taken limiting the choice to a single value. Indeed, the approximate function $\hat{u}(x)$ will be typically used to provide the value of the unknown function $u(x)$ and its derivatives in only specific regions within each interpolation domain. For instance by using point collocation we may limit the validity of the interpolation to a single point x_i. It is precisely in this context where we have found this meshless method to be more useful for practical purposes [10–13].

1.2 Discretization of governing equations

Let us assume a problem governed by the following set of differential equations

$$A(u_j) = 0 \qquad \text{in } \Omega \tag{13a}$$

with boundary conditions

$$u_j - \bar{u}_j = 0 \qquad \text{on } \Gamma_u \tag{13b}$$

$$B(u_j) = 0 \qquad \text{on } \Gamma_t \tag{13c}$$

In above A is a differential operator defining the governing differential equations to be satisfied on the domain Ω with boundary $\Gamma = \Gamma_t \cup \Gamma_\phi$, B is the differential operator defining the boundary conditions at the Neumann boundary Γ_t, u_j are the unknown variables with prescribed values $\bar{u}_j$ at the boundary Γ_u, $j = 1, 2, \cdots, N_v$ where N_v is the number of variables. In solid mechanics application u_j are the displacements and A and B are the equilibrium equations to be satisfied in the domain Ω and the boundary Γ_t where tractions are prescribed respectiveley.

The successful application of the FPM in fluid and solid mechanics requires the "stabilization" of the discrete form. The reasons for this stabilization in fluid problems is due to

the effect of convection terms and the need to satisfy the incompressibility requirements are due to the need for improving the satisfaction of the equilibrium equations (13a) and (13c) over a "cloud" when using a point collocation procedure.

A stabilized form of the differential equations [(13) can be found by using the *finite increment calculus* (FIC) procedure described in [14–17]. The FIC method is based on imposing the balance laws typical of solid and fluid mechanics over a domain of finite size and retaining higher order terms in the standard Taylor series expansion used to approximate the unknown field over the balance domain. The stabilized form of eqs. (13) reads

$$\begin{aligned} A - \underline{\frac{1}{2} h_j \frac{\partial A}{\partial x_j}} &= 0 \qquad \text{in } \Omega \\ u_j - \bar{u}_j &= 0 \qquad \text{on } \Gamma_u \\ B - \underline{\frac{1}{2} h_j n_j A} &= 0 \qquad \text{on } \Gamma_t \end{aligned} \tag{14}$$

where n_j are the components of the unit normal to the boundary Γ_t and h_j are the dimensions of the balance domain (also called characteristic length parameters). The underlined terms in eq.(14) introduce the necessary stabilization in the governing equations at discrete level. It can be shown that eqs.(14) are the starting point for deriving many well known stabilized numerical methods typically used in computational fluid dynamic problems [14–17]. The stabilized equations (14) have also been found useful for enhanced application of the FPM in fluid mechanics [12,13]. The efficiency of this stabilization procedure for the application of the FPM in solid mechanics will be shown in the examples presented in next section.

The discretized system of equations in the FPM is found by substituting the approximation (8) into eqs.(14) and *collocating* the differential equations at each point in the analysis domain. This gives

$$\begin{aligned} &\left[A(\hat{u}_j) - \frac{1}{2} h_j \frac{\partial}{\partial x_j} A(\hat{u}_j) \right]_k = 0 \qquad k = 1, 2 \cdots N_t \\ &[\hat{u}_j]_s - \bar{u}_j = 0 \qquad s = 1, 2 \cdots N_s \\ &\left[B(\hat{u}_j) - \frac{1}{2} h_j n_j A(\hat{u}_j) \right]_p = 0 \qquad p = 1, 2 \cdots N_t \end{aligned} \tag{15}$$

In above N_t is the number of points within the domain Ω and N_s and N_t are the points located on the boundaries Γ_u and Γ_t, respectively.

The discretized system of equations (15) can be written in the standard matrix form

$$\mathbf{K}\mathbf{u}^h = \mathbf{f} \tag{16}$$

from where the values of the nodal parameters u_i^h can be found.

Details of the implementation of the boundary conditions on the Dirichlet boundary Γ_t are given in [11,12].

The computation of the characteristic length parameters h_i follows the procedure explained in [13–17]. In the examples shown in the paper using quadratic base functions, the value $h_i = d_i^{\min}$ has been chosen where $d_i^{\min}$ is the closest distance from a star node in a cloud to its closest neighbour.

Further details on the FPM can be found in [10–13].

1.3 Example 1. Analysis of a simple supported beam under distributed loading

Figure 2 shows the geometry of the beam, the mechanical properties and the uniform distribution of 51 points. A uniform load acting on the upper edge is considered. A quadratic interpolation ($m = 6$) for the displacement variables has been chosen. Numerical results for the beam deflection and the horizontal stress distribution are shown. The same problem has been analyzed with the FEM using a structured mesh of 68 linear plane stress triangles (CST element) based on the same point distribution. Nodal stresses have been obtained by standard nodal averaging of element values. Comparison of the errors for the control deflection and the maximum σ_x stress gives some advantage to the stabilized FPM results (see Table 1).

Numerical results for grid of 51 points (68 CST finite elements)			
Central deflection error		Error in maximum σ_x stress	
FPM+S	FEM	FPM+S	FEM
19%	21%	19%	38%

Table 1: Simple supported beam. Numerical results for grid of 51 points (68 CST finite elements)

The convergence of the maximum horizontal stress and the maximum deflection value with the number of points is shown in the lower part of Figure 2, respectively. Results, listed as FPM+S, correspond to those obtained with the stabilized FPM described in the paper, whereas those listed as FPM were obtained neglecting the stabilization terms (i.e. the terms involving the characteristic lenght parameters in eqs.(14) and (15)). Note the benefitial effect of the stabilization terms leading to results which are more accurate than those obtained by the standard FEM in all cases.

1.4 Example 2. Square plate with circular hole under tension

Figure 3 shows the geometry of the plate and the loading. One quater of the plate is analyzed only due to symmetry. The problem has been solved with the FPM using two unstructured grids of 36 and 60 points. Contours of horizontal stress obtained with the stabilized FPM are shown in Figures 3 and 4 for the two grids. Results for the maximum horizontal stress at the upper tip of the hole obtained with the stabilized FPM are very accurate. This compares very favourably with the error obtained with the FEM using an unstructured mesh of CST elements. The distribution of the maximum horizontal stress along the line $x = 0$ is also shown in Figure 3 for the two grids studied. Note the greater accuracy of the stabilized FPM solution versus the standard FPM and FEM solutions (see Table 2).

36 points - 50 CST Triangles		60 points - 94 CST Triangles	
FPM+S	FEM	FPM+S	FEM
6%	38%	1,5%	21%

Table 2: Square plate with circular hole. Error in maximum horizontal stress obtained with the stabilized finite point method (FPM+S) and the finite element method (FEM)

CONCLUSIONS

The stabilized FPM is a promising numerical method for the meshless solution of problems in solid mechanics. Results for the two problems analyzed with the stabilized FPM yielded a higher accuracy than those obtained with standard FEM. The accuracy was remarkably higher for the maximum stress values. The optimal selection of the stabilization parameters and the validation of the stabilized FPM for problems involving heterogeneous materials and 3D geometries are the main challenges in the extension and validation of the new meshless procedure.

References

[1] J.J. Monaghan. *Smoothed particle hydrodynamics: Some recent improvement and applications.* Annu. Rev. Astron. Physics, **30**, 543, (1992).

[2] P.W. Randles and L.D. Libersky. *Smoothed particle hydrodynamics: Some recent improvement and applications.* Appl. Mech. Engng., **139**, 175, (1996).

[3] N. Perrone and R. Kao. *A general finite difference method for arbitrary meshes.* Comp. Struct, **5**, 45-47, (1975).

[4] T. Liszka and J. Orkisz. *The finite difference method at arbitrary irregular grids and its application in applied mechanics.* Comp. Struct., **11**, 83-95, (1980).

[5] B. Nayroles, G. Touzot and P. Villon. *Generalizing the FEM: Diffuse approximation and diffuse elements.* Comput. Mechanics, **10**, 307-18, (1992).

[6] T. BELYTSCHKO, Y. LU and L. GU. *Element free Galerkin methods.* Int. J. Num. Meth. Engng., **37**, 229-56, (1994).

[7] J. Dolbow and T. Belytschko. *An introduction to programming the meshless element free Galerkin method.* Archives of Comput. Meth. in Engng., **5** (3), 207–241, (1998).

[8] W.K. Liu, S. Jun, S. LI, J. Adee and T. Belytschko. *Reproducing Kernel particle methods for structural dynamics.* Int. J. Num. Meth. Engng., **38**, 1655–1679, (1995).

[9] W.K. Liu, Y Chen, s. Jun, J.s. Chen, T. Belytschko, C. Pan, R.A. Uras and C.T. Chang. *Overview and applications of the Reproducing Kernel particle method.* Archives of Comput. Meth. in Engng., Vol. **3**(1), 3–80, (1996).

[10] E. Oñate, S. Idelsohn, O.C. Zienkiewicz and T. Fisher. *A finite point method for analysis of fluid flow problems.* Proceedings of the 9th Int. Conference on Finite Element Methods in Fluids, Venize, Italy, 15-21, October (1995).

[11] E. Oñate, S. Idelsohn, O.C. Zienkiewicz and R.L. Taylor. *A finite point method in computational mechanics. Applications to convective transport and fluid flow.* Int. J. Num. Meth. Engng., Vol. **39**, 3839–3866, (1996).

[12] E. Oñate, S. Idelsohn, O.C. Zienkiewicz and R.L. Taylor. *A stabilized finite point method for analysis of fluid mechanics's problems.* Comput. Meth. in Appl. Engng., Vol. **139**, 1-4, pp. 315–347, (1996).

[13] E. Oñate and S. Idelsohn. *A mesh free finite point method for advective-diffusive transport and fluid flow problems.* Computational Mechanics, **21**, 283–292, (1988).

[14] E. Oñate. *Derivation of stabilized equations for advective-diffusive transport and fluid flow problems.* Comput. Meth. Appl. Mech. Engng., Vol. 151, 1-2, pp. 233–267, (1998).

[15] E. Oñate, J. García and S. Idelsohn. *Computation of the stabilization parameter for the finite element solution of advective-diffusive problems.* Int. J. Num. Meth. Fluids, Vol. 25, pp. 1385–1407, (1997).

[16] E. Oñate, J. García and S. Idelsohn. *An Alpha-adaptive approach for stabilized finite element solution of advective-diffusive problems with sharp gradients.* New Adv. in Adaptive Comp. Met. in Mech., P. Ladeveze and J.T. Oden (Eds.), Elsevier, (1998).

[17] E. Oñate. *A finite element method for incompressible viscous flows using a finite increment calculus formulation.* Research Report N. 150, CIMNE, Barcelona, January (1999).

[18] O.C. Zienkiewicz and R.L. Taylor. *The finite element method.* 4th Edition, Vol. 1, McGraw Hill, (1989).

[19] S.P. Timoshenko and J.N. Goodier. *Theory of elasticity.* 3rd. Edition, McGraw Hill, (1970).